

# Effects of electric field on the electronic structure and optical properties of quantum rods with wurtzite structure

Xin-Zheng Li and Jian-Bai Xia

Chinese Center of Advanced Science and Technology (World Laboratory), P.O. Box 8730, Beijing 100080, China  
and Institute of Semiconductors, Chinese Academy of Sciences, P. O. Box 912, Beijing 100083, People's Republic of China

(Received 15 November 2002; revised manuscript received 14 April 2003; published 16 October 2003)

The Hamiltonian of wurtzite quantum rods with an ellipsoidal boundary under electric field is given after a coordinate transformation. The electronic structure and optical properties are studied in the framework of the effective-mass envelope-function theory. The quantum-confined Stark effect is illustrated by studying the change of the electronic structures under electric field. The transition probabilities between the electron and hole states decrease sharply with the increase of the electric field. The polarization factor increases with the increase of the electric field. Effects of the electric field and the shape of the rods on the exciton effect are also investigated. The exciton binding energy decreases with the increase of both the electric field and the aspect ratio. In the end, considering the exciton binding energy, we calculated the band gap variation of size- and shape-controlled colloidal CdSe quantum rods, which is in good agreement with experimental results.

DOI: 10.1103/PhysRevB.68.165316

PACS number(s): 73.61.Ga, 78.66.Hf

## I. INTRODUCTION

Ever since the shape controlled colloidal quantum rods were achieved by modifying the synthesis,<sup>1,2</sup> such nanostructures have become a major subject of attention because of the freedom it offers in tailoring the materials and its much wider range of applications, such as biological labeling<sup>3,4</sup> and optoelectronic devices.<sup>5</sup> The electronic structures, optical properties, and linearly polarized emission of the quantum rods have already been studied systematically. For example, Hu *et al.*<sup>1</sup> studied the electronic structure of the colloidal quantum rods in the framework of the empirical pseudopotential theory and predicted and observed the linearly polarized emission of them. Li and Xia<sup>6</sup> studied the electronic structure and optical properties of the same quantum rods and explained the polarized emission in the framework of effective-mass envelope-function theory. A size-dependent optical spectroscopy was measured and studied by David Katz *et al.*<sup>7</sup> But until now, effects of the electric field on these properties have never been considered.

On the other hand, the effects of the electric field have been studied for quantum dots of other shapes such as spheres and cylinders. The effects of electric field on the electronic structure of a semiconductor quantum dot were investigated by Chang and Xia.<sup>8</sup> A selection rule for the optical transition between the conduction band and valence band states was given and the exciton binding energies were calculated as functions of the quantum dot radius and the strength of the electric field. Quantum-confined Stark effects of InAs/GaAs self-assembled quantum dots were studied by Li and Xia<sup>9</sup> in the framework of effective-mass envelope-function theory. The quantum dot was taken as a cylinder in their calculation and the redshift of the optical transition energies and energy difference between the ground state and the first excited state were given as functions of the electric field applied in a different direction. Still, the effects of the electric field on quantum dots are very important for applications.

Size- and shape-dependent electronic and optical properties of colloidal quantum rods are also very important. Band gap variation with the size and shape is an important aspect in both physics and applications. Li and Alivisatos measured the band gap energy of CdSe quantum rods with different widths and lengths in Ref. 10. Systematic discussions and a fitting surface are also given in that paper.

Motivated by these, we studied the effect of the electric field on the electronic structures and optical properties of CdSe quantum rods with wurtzite structure in the framework of the effective-mass envelope-function theory. The effects of the electric field and the shape of the rods on the exciton effect are also investigated with this method. Still, considering the exciton binding energy, the band gap variations with size and shape of the quantum rods are investigated and compared with experimental results. The theoretical model is given in Sec. II. The energies of both the electron and hole ground states decrease with the increase of the electric field. The electric field potential item contributes negatively since the electron and hole tend to float along its direction in the confined district. A quantum-confined Stark effect is clearly indicated by these facts. The changes of the transition probabilities and the polarization factor with electric field are investigated. We further studied the effects of the electric field and the shape of the rods on the exciton effect. It is found that the exciton binding energy decreases sharply with the increase of the aspect ratio of the quantum rods and the electric field strength. Also, the band gap variation of the size- and shape-controlled colloidal CdSe quantum is calculated. These discussions and results are given in Sec. III. Finally, we draw a brief conclusion in Sec. IV.

## II. MODEL AND CALCULATION

### A. Electronic structure and oscillator strength of optical transition

For wurtzite structure CdSe quantum rods, the  $z$  axis is the long axis. We assume the electric-field strength vector as follows:

$$\mathbf{E} = E_{\text{QR}}(\cos \theta_1 \mathbf{k} + \sin \theta_1 \cos \varphi_1 \mathbf{i} + \sin \theta_1 \sin \varphi_1 \mathbf{j}). \quad (1)$$

Since it is symmetric along the  $z$  axis, we can take  $\varphi_1$  as 0 in the calculation. Then the electric field potential term in the Hamiltonian for the hole and electron can be simplified as follows:

$$V(\mathbf{r}_h) = -e\mathbf{E} \cdot \mathbf{r}_h = -eE_{\text{QR}}r_h(\cos \theta_1 \cos \theta + \sin \theta_1 \sin \theta \cos \varphi), \quad (2)$$

$$V(\mathbf{r}_e) = e\mathbf{E} \cdot \mathbf{r}_e = eE_{\text{QR}}r_e(\cos \theta_1 \cos \theta + \sin \theta_1 \sin \theta \cos \varphi). \quad (3)$$

For our cases of quantum rods, we take the boundary condition as elliptic and assume an infinite barrier. In order to simplify it into that of the spherical case which has a better symmetrical characteristic,<sup>11–15</sup> we use the coordinate transformation which can transform the boundary into a spherical one in a new coordinate system introduced in Ref. 6,  $x' = x$ ,  $y' = y$ ,  $z' = z/e'$ , where  $e'$  is the aspect ratio of the ellipsoid,  $x, y, z$  are the actual coordinates, and  $x', y', z'$  are the transformed ones. The total Hamiltonian for the hole state is the summation of the Hamiltonian with zero spin-orbital coupling (SOC), the spin-orbital coupling Hamiltonian, and the electric field term. The hole and electron Hamiltonians in the transformed coordinate system and the spin-orbital coupling Hamiltonian are given in Ref. 6.

The electric field potential term for the hole is written as

$$V(\mathbf{r}_h) = -e\mathbf{E} \cdot \mathbf{r}_h = -eE_{\text{QR}}r'_h(e' \cos \theta_1 \cos \theta' + \sin \theta_1 \sin \theta' \cos \varphi') \quad (4)$$

in the new coordinate system, where  $r'_h$  is the transformed radius. That for the electron is written as

$$V(\mathbf{r}_e) = eE_{\text{QR}}r'_e(e' \cos \theta_1 \cos \theta' + \sin \theta_1 \sin \theta' \cos \varphi') \quad (5)$$

in the new coordinate system, the boundary is spherical, so we expand the radial part with Bessel functions and the angle part with spheric harmonic functions as in Ref. 6.

To simplify the calculation, we use the spheric harmonic function to describe the electric field Hamiltonian term

$$V(\mathbf{r}) = -qe'E_{\text{QR}}R \cos \theta_1 (r'/R)(4\pi/3)^{1/2}Y_{1,0} - qE_{\text{QR}}R \sin \theta_1 (2\pi/3)^{1/2}(Y_{1,-1} - Y_{1,1}), \quad (6)$$

where  $q$  is  $e$  for holes and  $-e$  for electrons and  $R$  is the transverse radius. Since the second term in the above equation will couple states with different  $m$ , for simplicity we only consider the case of the electric field along the  $z$  axis in the following, i.e.,  $\theta_1 = 0$ . We use two parameters  $K'$  and  $K$  defined as follows to represent the electric field strength in the calculations of the hole states and electron states, respectively:

$$K' = \frac{ee'E_{\text{QR}}R}{\frac{\gamma_1}{2m_0} \left(\frac{\hbar}{R}\right)^2},$$

$$K = \frac{ee'E_{\text{QR}}R}{\frac{1}{2m_x} \left(\frac{\hbar}{R}\right)^2}. \quad (7)$$

In the above descriptions,  $E_{\text{QR}}$  is the electric field strength in the quantum rods, not  $E_{\text{ext}}$ , the actual electric field applied. The relation  $E_{\text{QR}}$  and  $E_{\text{ext}}$  for the spherical case is described in Refs. 8,16–18. For the elliptic case, the relation is rather complicated. We simply list the relations as

$$E_{\text{QR}} = \frac{\epsilon_2}{\epsilon_1 n^{(2)} + (1 - n^{(2)})\epsilon_2} E_{\text{ext}},$$

$$n^{(2)} = \frac{1 - e^2}{2e^2} \left( \ln \frac{1 + e}{1 - e} - 2e \right), \quad (8)$$

where  $\epsilon_1$  is the dielectric constant of CdSe and  $\epsilon_2$  is that of its surrounding materials. Since the main purpose of this article is to study the effect of the electric field on the electronic structure and optical properties of quantum rods, we directly take  $K'$  and  $K$  as parameters.

By solving the effective-mass equation in which we ignored the exciton effect at first, we can calculate the energies of electron and hole states and the oscillator strength of the optical transition following the method given in Ref. 14. Because of the ellipsoid symmetry, only the  $z$  component of the angular momentum is the good quantum number. For an electron it is  $L_z$  and for a hole it is  $J_z (J = L + S, S = 3/2)$ .

## B. Exciton effect

We take the exciton effect into account by adding the Coulomb interaction between the electron and hole into the Hamiltonian given above as a perturbation because the size of the quantum rods is much smaller than the exciton radius  $\mathbf{a}_B$ . The Coulomb interaction term between the electron and hole can be written as

$$V_{e-h} = -\frac{e^2}{\epsilon_r r_{eh}}. \quad (9)$$

The matrix element of the Coulomb interaction can be calculated by using

$$\frac{1}{r_{eh}} = -\sum_{k=0}^{\infty} \frac{r_{<}^k}{r_{>}^{k+1}} P_k(\cos \theta_{eh}), \quad (10)$$

$$P_k(\cos \theta_{eh}) = \frac{4\pi}{2k+1} \sum_{m=-k}^k Y_{km}^*(\theta_e, \varphi_e) Y_{km}(\theta_h, \varphi_h), \quad (11)$$

where  $r, \theta$ , and  $\varphi$  are the real coordinates of the system,  $P_k$  is the Legendre polynomial  $\theta_{eh}$  is the angle between the

TABLE I. Parameters for CdSe in the actual calculation (from Ref. 6). See Ref. 16.

$m_x$	$m_z$	$\gamma_1$	$\gamma_2$	$\gamma_2'$	$\gamma$	$\gamma_1'$	$\gamma_3'$	$A$	$\Delta_c$ (meV)	$\lambda$ (meV)
0.1756	0.1728	1.7985	0.7135	0.7970	1.4492	2.166	0.3779	0.6532	25	-139.3

position vectors of electron ( $\mathbf{r}_e$ ) and hole ( $\mathbf{r}_h$ ),  $r_< = \min(r_e, r_h)$ , and  $r_> = \max(r_e, r_h)$ .<sup>15</sup>

With the model given in the above subsection, we can get the energy states and the wave functions of both the electrons and the holes. The wave function is written by the transformed coordinates which are represented by  $r'$ ,  $\theta'$ , and  $\varphi'$ . For a specific optical transition from one electron state  $i$  to one hole state  $j$ , the exciton energy can be calculated by the following equation:

$$\langle V_{e-h} \rangle = \langle \psi_{ei} \psi_{hj} | V_{e-h} | \psi_{ei} \psi_{hj} \rangle, \quad (12)$$

where  $\psi_e$  and  $\psi_h$  are represented by  $r'$ ,  $\theta'$ , and  $\varphi'$ , while  $V_{e-h}$  is written in the real coordinate system. We can use the relationships between the real coordinates and the transformed ones as follows to do our calculation:

$$\cos \theta' = \frac{\cos \theta}{\sqrt{e^2 + (1 - e^2) \cos^2 \theta}},$$

$$r' = r \sqrt{1 + \left( \frac{1}{e^2} - 1 \right) \cos^2 \theta}. \quad (13)$$

The integration of Eq. (12) is done in the real coordinate system for an exciton state.

### III. RESULTS AND DISCUSSIONS

#### A. Electronic states

We use the effective mass parameters for CdSe given in Table I and take  $R=2.1$  nm and the aspect ratio  $e'$  as 2.

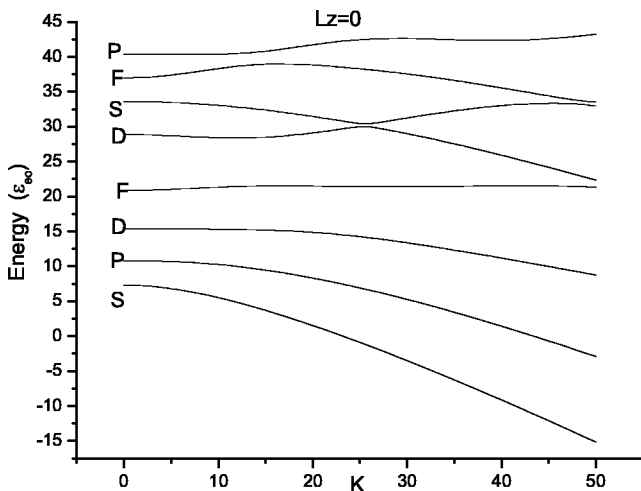


FIG. 1. Energies of the  $L_z=0$  electronic state with respect to the bottom of the conduction band of quantum ellipsoids as functions of  $K$ , in units of  $\epsilon_{e0} = (1/2m_x)(\hbar/R)^2$  for  $e' = 2$ .

Figure 1 shows the energies of the  $L_z=0$  electron states as functions of the electric field applied. Figure 2 shows that of the  $L_z=1$  states. The signals  $S$ ,  $P$ ,  $D$  of each line represent the main component of each wave function for the zero electric field case. As we can see from Eq. (6), different from that of the electronic structure without the electric field applied, the electric field term includes a  $Y_{10}$  term in the Hamiltonian, which will couple both the  $l$  and  $l+1$  components of the electronic wave function. From both Figs. 1 and 2, for the ground and low excited states, energy decreases with the increase of the electric field. Physically, this is because the electric field produces a potential well in the  $z$  direction of the quantum rod, resulting in a decrease of the energies of low lying states (quantum confined Stark effect). The unit of the electric field strength  $K$  is dimensionless [see Eq. (7)]. From Fig. 1 we see that the energy of the ground state  $S$  decreases to zero (the conduction band bottom) at  $K=23$ . From Eq. (7), for a constant  $K$ , the electric field strength  $E_{QR}$  is inversely proportional to the aspect ratio  $e'$  and the third power of the transverse radius  $R$ , so the larger the  $R$  and  $e'$ , especially  $R$ , the stronger the effect of the electric field. If we compare these two figures carefully, we find that the  $S$  state decreases quickly with  $K$  in Fig. 1, which is followed by that of the  $P$  states in both figures. This tallies quite well with the result given in Ref. 8. The first  $D$  state decreases slightly with  $K$  and the second  $D$  state waves in both figures. This is due to the orthogonality of the excited state to the ground state. We also take out the datum of the first  $P$  and  $D$  state to compare the effect of the electric field on the state with the same  $l$  and a different  $L_z$ . In Fig. 3, we see that for both  $P$  and  $D$  states, the energy for the  $L_z=1$  state always decreases faster. This is because  $L_z=0$  states mainly extend in the  $z$  direction, while the  $L_z=1$  states mainly extend in the  $x$ - $y$

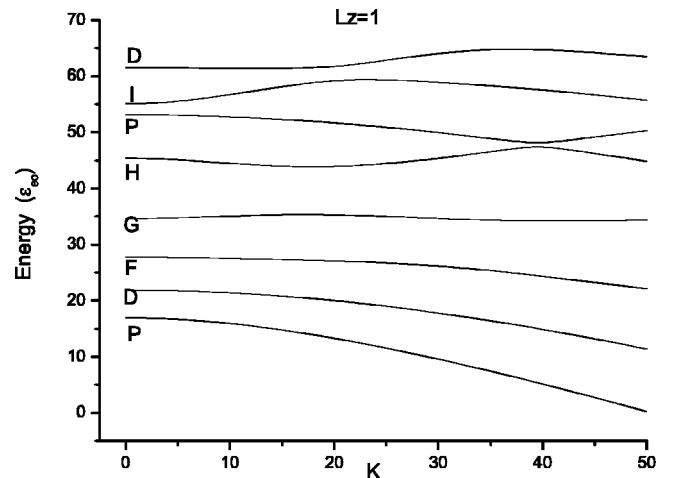


FIG. 2. Energies of the  $L_z=1$  electronic state with respect to the bottom of the conduction band of quantum ellipsoids as functions of  $K$ , in units of  $\epsilon_{e0} = (1/2m_x)(\hbar/R)^2$  for  $e' = 2$ .

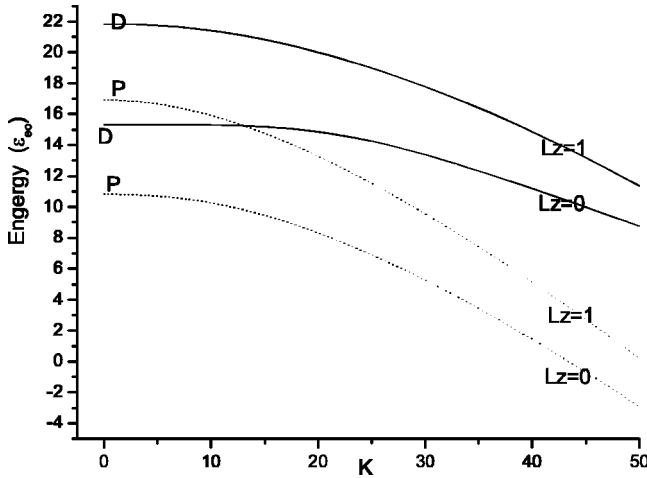


FIG. 3. Energies of  $L_z=0$  and 1 of  $P$  and  $D$  states with respect to the bottom of the conduction band of quantum ellipsoids as functions of  $K$ , in units of  $\epsilon_{e0}=(1/2m_x)(\hbar/R)^2$  for  $e'=2$ . The  $P$  states are represented by dotted curves and  $D$  states are represented by solid curves.

directions. The  $L_z=1$  states shifts to the one end of the rod in the electric field more strongly than the  $L_z=0$  state.

**B. Hole states**

Figure 4 shows the effect of the electric field on the  $J_z=1/2$  hole states. The signal of each curve represents the main component of its wave function. The energies are calculated from the top of the valence band downwards. For the same reason discussed above, the hole energies also decrease with the increase of  $K'$ . Figure 5 shows the same for the

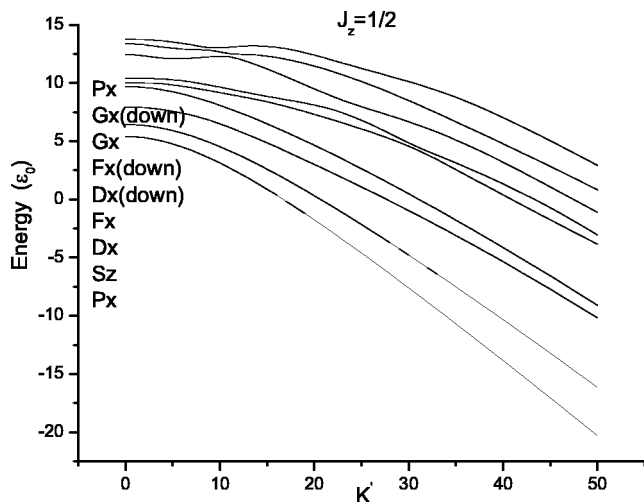


FIG. 4. Energies of the  $J_z=1/2$  hole state with respect to the top of the valence band of quantum ellipsoids as functions of  $K'$ , in units of  $\epsilon_0=(\gamma_1/2m_0)(\hbar/R)^2$  for  $R=2.1$  nm and  $e'=2$ . The labels represent the characteristics of the hole states in order from up to down, respectively.  $S, P, D$  represents the major component of each wave function for the zero electric field case. Indexes  $x$  and  $z$  represent that the basic function of the envelope function is an  $x$ - or  $z$ -like Bloch function at the top of the valence band. “Down” means down spin while no label means up spin.

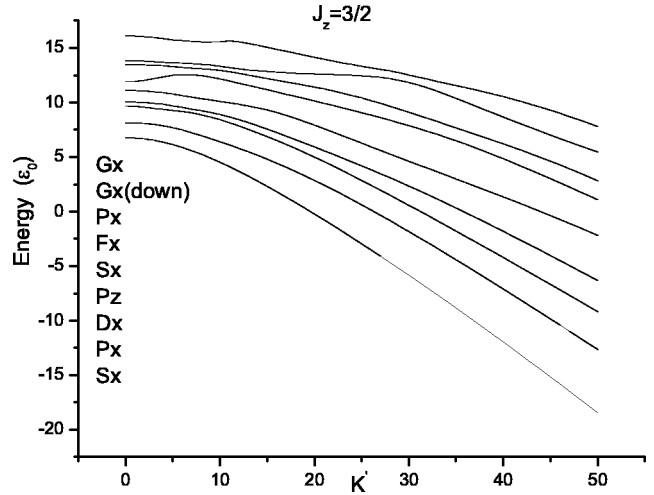


FIG. 5. Energies of the  $J_z=3/2$  hole state with respect to the top of the valence band of quantum ellipsoids as functions of  $K'$ , in units of  $\epsilon_0=\gamma_1/2m_0(\hbar/R)^2$  for  $R=2.1$  nm and  $e'=2$ . The meaning of the labels is the same as in Fig. 4.

$J_z=3/2$  hole states. From these two figures and that of the electrons above, we can see that the band gap decrease clearly with the increase of the electric field.

**C. Transition probabilities**

Figures 6 and 7 show the total transition probabilities from the first  $L_z=0$  electron state to the first five  $J_z=1/2$  and  $J_z=3/2$  hole states as functions of  $K'$ , respectively. In the calculation, for every transition, we calculated the transition probabilities along the  $x$  and  $z$  directions, respectively. They are different from the equations we used in Ref. 6, because the first  $L_z=0$  electron state is comprised of both even and odd  $l$  components. The transition probability is proportional to

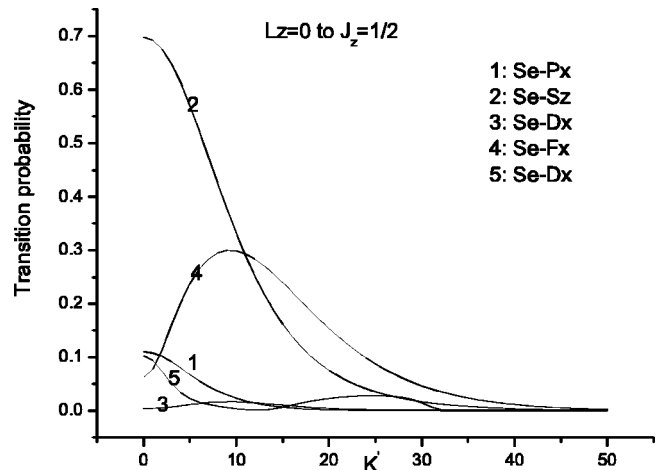


FIG. 6. Total optical transition probability from the first  $L_z=0$  electronic state to the first five  $J_z=1/2$  hole states (labeled as in Figs. 1–5) as functions of  $K'$ .  $S_e$  is the basic electron state and its major component is the  $S$  state.  $P_x, S_z$ , etc. are hole states, as in Fig. 4.

$$|\langle \psi_e | \psi_{\frac{1}{2}}^1 \rangle|^2 = \begin{cases} \left[ \sum_{n,l=0,2,4} e_{ln} b_{ln} \right]^2 + \left[ \sum_{n,l=1,3,5} e_{ln} f'_{ln} \right]^2 & z \text{ polarization,} \\ \left[ \sum_{n,l=0,2,4} e_{ln} a'_{ln} \right]^2 + \left[ \sum_{n,l=0,2,4} e_{ln} d_{ln} \right]^2 & x+y \text{ polarization,} \end{cases} \quad (14)$$

and

$$|\langle \psi_e | \psi_{\frac{3}{2}}^3 \rangle|^2 = \left[ \sum_{n,l=0,2,4} e_{ln} a_{ln} \right]^2 + \left[ \sum_{n,l=1,3,5} e_{ln} d'_{ln} \right]^2 \quad x+y \text{ polarization.} \quad (15)$$

where the coefficients are defined in Ref. 6.

The total transition is the summation of all contributions of  $z$ ,  $x$ , and  $y$  polarizations. From these two figures, we see that the transition decreases with the increase of the electric field applied. These can be easily understood since the electric field draws the electrons and holes in different directions spatially. From this aspect, we can see that an important effect of the electric field on the optical properties of the quantum rod is to decrease its transition probabilities which is negative for optoelectronic applications.

#### D. Polarization of the emission

We further studied the effect of the electric field on the polarization factor of the emission. Figure 8(a) shows the polarization factor as a function of  $K'$ . In all the above calculations, we took the aspect ratio of the quantum rods as 2. Figure 8(b) shows the polarization factor as a function of  $K'$  for the  $e'=3$  case. Without an electric field, the polarization factor for  $e'=3$  case is larger than that of the  $e'=2$  case. This follows the rule we discussed in Ref. 6. With the increase of the electric field, in addition to the decrease of  $I_z$

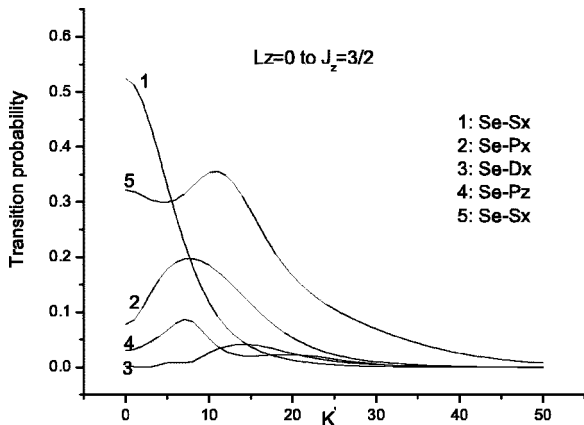


FIG. 7. Total optical transition probability from the first  $L_z=0$  electronic state to the first five  $J_z=3/2$  hole states as functions of  $K'$ .

and  $I_x$  which was discussed in the above paragraph, we also found an increase of the polarization factor in both figures. A clear explanation of this phenomenon requires an overall investigation of the energy state and envelope functions as we did in Ref. 6. We can simply describe it in the following way. Since the electric field is along the  $z$  direction, the wave functions along the  $(x-y)$  directions will be affected more strongly than those along the  $z$  direction.  $I_x$  decreases faster than  $I_z$  and the polarization factor  $P$  increases. This phenomenon is very meaningful for the application of such quantum rods.

#### E. Exciton effect

We also studied the effects of the electric field and the shape of the rods on the exciton effect. We calculated the exciton binding energy of the ground exciton state. The result is given in Fig. 9. From the figure we can see that the exciton binding energy decreases with the electric field. This

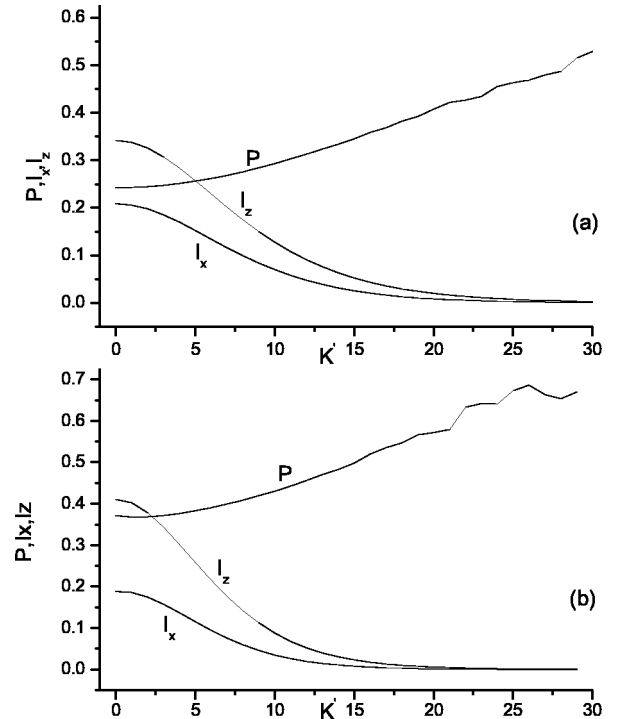


FIG. 8. (a) Polarization factor of the emission as functions of  $K'$  when  $e'=2$  and  $R=2.1$  nm.  $I_x$  represents the total transition probability calculated by Eqs. (14) and (15) when the polarization is along the  $x$  axis.  $I_z$  indicates that when the polarization is along the  $z$  axis.  $P$  represents the polarization factor of the emission. (b) Polarization factor of the emission as functions of  $K'$  when  $e'=3$  and  $R=2.1$  nm.

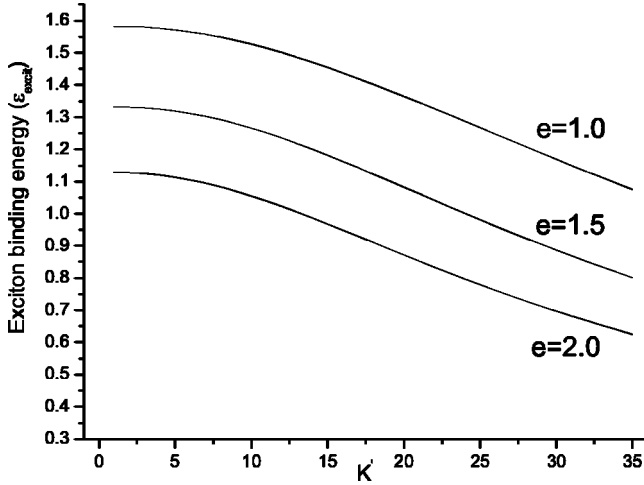


FIG. 9. The exciton binding energy as a function of  $K'$  for the quantum rods with aspect ratio  $e' = 1.0, 1.5,$  and  $2.0,$  respectively, in units of  $\epsilon_{\text{excit}} = e^2/\epsilon_r R.$

is because the electron and hole tend to drift toward opposite directions along the  $z$  axis, so the Coulomb interaction between them decreases. The stronger the electric field applied, the farther the electrons and holes are separated, the weaker the Coulomb interaction, and the smaller the exciton binding energy. The figure also indicates that the exciton binding energy decreases with the increase of the aspect ratio of the quantum rods. We can describe this from the same point of view. For quantum rods with a larger aspect ratio, compared to those of the smaller  $e'$  case, the electrons and holes are less confined and the space available for their movement is bigger, so the average distance between the electron and hole is larger which necessarily leads to a decrease of the Coulomb interaction and a weaker exciton energy.

#### F. Band gap

Still taking the boundary barrier as infinity, considering the exciton binding energy this time, we calculated the band gap energy as functions of the width and length of the quantum rods. The result is given in Table II. The  $PL(eV)$  column in the table gives the experiment datum of the  $T = 295$  K cases in Ref. 10.  $E_e$  and  $E_h$  represent the energy of the first electron state and the first hole state, respectively.  $E_{\text{ex}}$  represents the exciton binding energy of this electron-hole pair. The last column lists the band gap calculated this way. Compared with the results in Ref. 6, these datum fit the experiment datum given in Ref. 10 better. This is because we considered the exciton binding energy this time. The band gap is still a little bigger than the experiment data especially for the little rods. For the large-size cases, this difference is smaller. This is because the boundary in our model is too sharp compared to the actual situation. The larger the width and length, the weaker the confinement, the smaller the differences between the boundary condition in the model and the actual cases, and the better the model fits the actual situation. For these reasons, the energy difference between the

TABLE II. Electronic structure of CdSe quantum rods with different widths and lengths.

Length (nm)	Width (nm)	PL (eV)	Electronic structure			Band gap (eV)
			$E_e(eV)$	$E_h(eV)$	$E_{\text{ex}}(eV)$	
11.0	3.2	2.20	0.5570	0.1170	0.0679	2.4624
11.5	3.6	2.17	0.4447	0.0963	0.0645	2.3328
7.6	3.7	2.16	0.4593	0.1312	0.0878	2.3590
9.2	3.7	2.19	0.4397	0.0976	0.0765	2.3171
8.6	3.8	2.12	0.4254	0.0958	0.0795	2.2980
9.7	4.0	2.12	0.3781	0.0571	0.0714	2.2487
11.6	4.0	2.18	0.3524	0.0817	0.0626	2.2278
13.4	4.1	2.13	0.3417	0.0762	0.0556	2.2186
20.2	4.2	2.02	0.3114	0.0687	0.0390	2.1974
8.7	4.3	2.07	0.3414	0.0803	0.0746	2.2034
8.6	4.4	2.10	0.3292	0.0782	0.0743	2.1894
31.5	4.4	1.98	0.2759	0.0610	0.0257	2.1675
15.3	4.5	2.10	0.2821	0.0644	0.0491	2.1537
12.4	4.8	2.03	0.2593	0.0615	0.0563	2.1208
18.4	4.9	2.06	0.2348	0.0548	0.0416	2.1043
12.0	5.1	1.99	0.2341	0.0571	0.0560	2.0915
11.4	5.2	2.00	0.2288	0.0565	0.0574	2.0842
40.8	5.3	1.90	0.1894	0.0447	0.0204	2.0700
8.5	5.5	1.95	0.2274	0.0594	0.0663	2.0768
23.6	5.5	1.97	0.1836	0.0445	0.0334	2.0510
14.0	6.2	1.94	0.1599	0.0421	0.0469	2.0114
17.6	6.4	1.93	0.1442	0.0380	0.0402	1.9983

results we obtained and the experiment data is smaller for quantum rods with larger widths and lengths.

#### IV. CONCLUSIONS

In this article, we studied the effect of the electric field on the electronic structures and optical properties of quantum rods with wurtzite structure using the effective-mass envelope function theory considering the spin-orbital coupling. The change of the electronic state energy with electric field was summarized to indicate the quantum confined Stark effect. In addition to a decrease of the transition probabilities with the electric field, a very interesting increase of the polarization factor was also found. The exciton effect was discussed. The exciton binding energy was found to decrease with the increase of both the electric field and the aspect ratio. Finally, band gap variation with the size and shape of the quantum rods was calculated considering the exciton binding energy. It was found to be in good agreement with experimental results. These phenomena were discussed and brief explanations were given.

#### ACKNOWLEDGMENTS

This work was supported by the National Natural Science Foundation of China, the special funds for Major State Basic Research Project No. G001CB3095 of China, and the project of Chinese Academy of Sciences *Nanometer Science and Technology*.

- <sup>1</sup>J.T. Hu, L.S. Li, W.D. Yang, L. Manna, L.W. Wang, and A.P. Alivisatos, *Science* **292**, 2060 (2001).
- <sup>2</sup>Shi-Hai Kan, Taleb Mokari, Eli Rothenberg, and Uri Banin, *Nat. Mater.* **2**, 155 (2003).
- <sup>3</sup>M. Bruchez, Jr., M. Moronne, P. Gin, S. Weiss, and S.P. Alivisatos, *Science* **281**, 2013 (1998).
- <sup>4</sup>W.C.W. Chan and S. Nie, *Science* **281**, 2016 (1998).
- <sup>5</sup>V.I. Klimov, A.A. Mikhailovsky, Su Xu, A. Malko, J.A. Hollingsworth, C.A. Leatherdale, H.J. Eisler, and M.G. Bawendi, *Science* **290**, 314 (2000).
- <sup>6</sup>X.Z. Li and J.B. Xia, *Phys. Rev. B* **66**, 115316 (2002).
- <sup>7</sup>David Katz, Tommer Wizansky, Oded Millo, Eli Rothenberg, Taleb Mokari, and Uri Banin, *Phys. Rev. Lett.* **89**, 086801 (2002).
- <sup>8</sup>K. Chang and J.B. Xia, *J. Appl. Phys.* **84**, 1454 (1998).
- <sup>9</sup>S.S. Li and J.B. Xia, *J. Appl. Phys.* **88**, 7171 (2000).
- <sup>10</sup>L.S. Li, J.T. Hu, W.D. Yang, and A.P. Alivisatos, *Nano Lett.* **1**, 349 (2001).
- <sup>11</sup>J.B. Xia and J.B. Li, *Phys. Rev. B* **60**, 11540 (1999).
- <sup>12</sup>J.B. Xia, *Phys. Rev. B* **40**, 8500 (1989).
- <sup>13</sup>J.B. Xia, *J. Lumin.* **70**, 120 (1996).
- <sup>14</sup>J.B. Li and J.B. Xia, *Phys. Rev. B* **61**, 15 880 (2000).
- <sup>15</sup>A. R. Edmonds, *Angular Momentum in Quantum Mechanics* (Princeton University Press, Princeton, NJ, 1957), p. 68.
- <sup>16</sup>The value of parameter  $A$  in Table I of Ref. 6 is not correct. It is listed as 1.7985 but should be 0.6532.
- <sup>17</sup>Al.L. Efros, M. Rosen, M. Kuno, M. Nirmal, D.J. Norris, and M. Bawendi, *Phys. Rev. B* **54**, 4843 (1996).
- <sup>18</sup>L. Genzel and T. Matin, *Surf. Sci.* **34**, 33 (1973).